International Journal of Smart Grid and Clean Energy

Applicability of fixed bed reactors for methanation in electrolysis-methanation-cells

Carsten Cosse, Stefan Best, and Detlef Schulz

Helmut-Schmidt-University / University of the Bundeswehr, Holstenhofweg 85, 22043 Hamburg, Germany

Abstract

With the increasing share of fluctuating power generation in the electrical grid energy storage systems with large capacities receive an increasing interest. Power-to-Gas in particular enables the storage of vast quantities of electrical energy over long periods. Especially methanation of the produced hydrogen allows an unlimited use of the existing infrastructure for natural gas, however, the overall efficiency of the process and the initial installation costs still prevent widespread application. In this paper a novel concept for a combined electrolysis-methanation-cell is presented, which aims at a reduced complexity of the system and an increased efficiency by utilising synergies between electrolysis and methanation. The requirements for the reactor in the electrolysis-methanation-cell are defined and a simulation for a fixed bed reactor in an electrolysis-methanation-cell is carried out. It is shown that a new type of reactor is needed to fulfil the presented requirements, due to the inherent characteristics of fixed bed reactors, which are not ideally suited for application in electrolysis-methanation-cells.

Keywords: Electrolysis; power-to-gas; methanation; electrolysis-methanation-cell

1. Introduction

Efficient and cost effective energy storage has become one of the most intensely studied fields of research over the past years. In order to ensure reliability for the supply of electrical energy, in a grid with an increasing share of generation from fluctuating sources, large energy stores are the only option. Especially when thinking about the balancing of large electrical grids, like the trans European-grid, the required storage capacities quickly exceed the order of magnitude in which electrochemical batteries are a suitable option. Since the natural gas grid (GG) includes strategic energy reserves sufficient for several months [1], Power-to-Gas (PtG) is one of the most promising concepts in the field of energy storage. Surplus electrical energy is used in an electrolyser to split water into hydrogen and oxygen gas.

$$2H_2O \rightarrow 2H_2+O_2 \tag{1}$$

Depending on the feed in location of the electrolyser, hydrogen gas can be stored in the GG up to a concentration of 5 Vol-% [2]. To remove this limitation of the storage capacity, hydrogen is converted into methane by adding carbon dioxide (CO_2) into a chemical reactor. This process is known as the Sabatier-reaction:

$$CO_2 + 4H_2 \rightarrow CH_4 + 2H_2O \qquad \Delta H^0 = -165 \text{ kJ/mol} \tag{2}$$

The produced methane gas is a full substitute for natural gas and can be fed into the GG without any restrictions regarding its concentration. Further, methane can be used in all sectors of the energy market and the GG is also able to facilitate transport of the energy from the place of generation to the place of consumption. Low energy efficiency and high costs prevent the widespread application of this technology.

* Manuscript received July 17, 2020; revised November 7, 2020.
Corresponding author. Tel.: +49 152 57578956; *E-mail address:* cosse@hsu-hh.d
doi: 10.12720/sgce.9.6.930-938

In Section 2 of this paper, a concept to improve PtG systems with a novel electrolysis-methanation-cell (EMC) is presented, detailing the expected advantages and the unique requirements for the integrated methanation reactor. In Section 3 a simulation of the most common reactor type is presented, giving an estimated performance for EMC with a conventional fixed bed reactor. In Section 4 the conclusions drawn from the presented simulation are given and a promising new type of reactor is introduced.

2. Concept: Electrolysis-Methanation-Cell

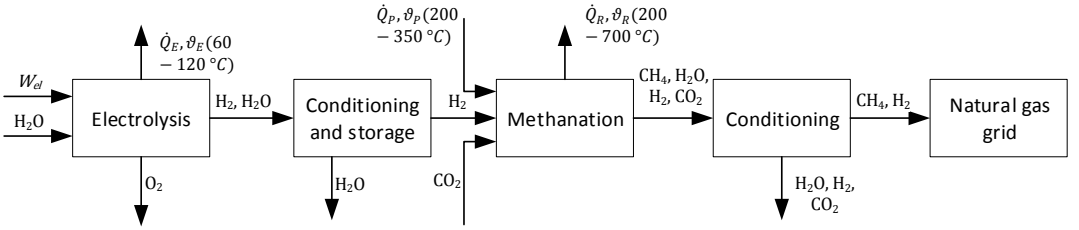

Fig. 1. Block diagram of a typical PtG process (modified from [3]).

In existing PtG plants electrolysis and methanation are realised in separate devices as shown in Fig. 1.

Intermediate storage between electrolysis and methanation prevents the utilisation of temperature synergies between the two processes and thus decreases the energy efficiency. In the proposed EMC, as patented in [3-6], the methanation reaction is realised in the exhaust channel of the electrolyser, eliminating storage and gas conditioning components between the two processes and thereby lowering the cost of the system. Fig. 2 (a) presents the block diagram of the process in an EMC and Fig. 2 (b) shows a schematic design of an integrated EMC.

2.1. Expected advantages of EMC

The direct integration of both processes, electrolysis and methanation, into one device leads to a more efficient coupling, as waste heat can be reused without additional components. This is expected to result in an increased efficiency of the system, which will lower the cost of PtG as energy storage. Further cost reductions are expected, since the simplified process will require less components and therefore less material and less space. Lastly direct integration and coupling of both processes can improve the transient behaviour of the methanation which will improve the ability of the system to compensate for fluctuating renewable energy generation.

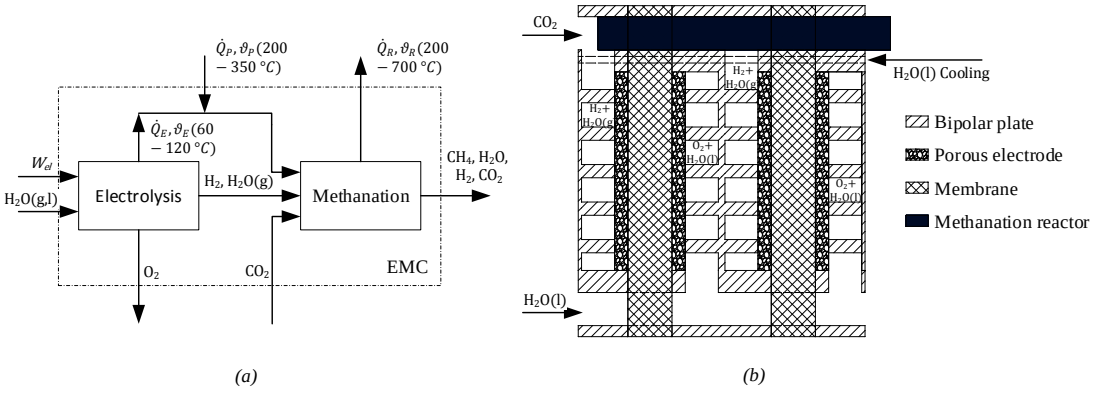

Fig. 2. (a) Block diagram of the thermochemical process inside an EMC (modified from [3]), (b) Schematic design of an integrated EMC.

2.2. Requirements for the reactor

Integration of the methanation reactor into an electrolyser leads to a number of requirements, which will be discussed in the following.

High gas hourly space velocity ($GHSV$>10,000 h^{-1}) with significant conversion (X_{CO2}>70 %). The limited size of the reactor due to the integration into the electrolyser leads to the requirement of a high gas hourly space velocity. To ensure almost complete conversion the EMC will be supplied with less CO_2 than the stoichiometric requirement. Further, different ways to introduce the CO_2 into the reactor are possible ranging from central nozzles to distributed introduction through porous filters. The residual concentration of CO_2 in the product gas of the EMC should be below 6 vol-%, the maximum concentration allowed in the GG [2] so that the gas conditioning unit between EMC and GG can be simplified.

Process stability is required under partial load and transient operation. Since PtG processes need to increase and decrease their power consumption with the fluctuation in the electric grid, a broad range of operation is required. Therefore, the efficiency of the system under partial load should not be diminished significantly compared to the optimal operating conditions. The given requirements on the gas mixture in [2] need to be kept, even during transient phases where the load of the system is changed.

The initial installation and operating costs for the EMC with the required reactor and ancillary systems should be below the costs of a comparable conventional system (Fig. 1). For example, the degradation of the catalyst is a factor to be taken into account.

Integration of the methanation reactor, and with that a source of heat, into the exhaust channel of the electrolyser should not affect the performance of the electrolyser. Therefore, the reactor needs to be cooled, or operated at the same temperature as the electrolyser. Cooling of the reactor should be done with either the water cycle of the electrolyser, the CO_2 gas or the electrolysis gas. Any combination of these options is also viable.

3. Simulation of a Fixed Bed Reactor

In the first part of this section a simulation model for the methanation reaction with Nickel catalyst particles on Alumina, based on Chein et al. [7], will be presented. In the second paragraph the simulated domain is characterised and the setup of the parameter study is explained. In the third paragraph the conversion performance of the fixed bed methanation reactors in EMC application as simulated by the presented model is visualised.

3.1. Simulation model

To simulate the behaviour of the reactor the transport phenomena inside the fixed bed need to be described with conservation equations for mass, momentum, energy and the chemical species. The following simplifying assumptions are used to formulate the model:

- Weakly compressible, steady, laminar flow (Brinkman-Darcy-Forchheimer model)
- Homogenous permeability and porosity of the bed, particles assumed spherical (Brinkman-Darcy-Forchheimer model)
- All species exhibit ideal gas behaviour
- Catalyst bed and fluid in thermal equilibrium

Therefore, the momentum balance can be written as:

$$\frac{\rho_f}{\epsilon_p^2}\nabla\vec{u}^2=\nabla\left[-p\mathbf{I}+\frac{\eta_f}{\epsilon_p}(\nabla\vec{u}+(\nabla\vec{u})^T)-\frac{2}{3}\frac{\eta_f}{\epsilon_p}(\nabla\vec{u})\mathbf{I}\right]-\left(\frac{\eta_f}{\kappa}+\frac{C_F\rho_f}{\sqrt{\kappa}}|\vec{u}|\right)\vec{u}. \quad (3)$$

With the additional requirement $\rho_f\nabla\vec{u}=0$. In (3) ρ_f is the fluid density, ϵ_p is the porosity of the bed, $\nabla\vec{u}$ is the gradient of the fluid velocity vector, p the pressure, $\mathbf{I}$ the unit matrix, η_f the fluid viscosity, κ the

permeability of the bed and C_F the Forchheimer coefficient. Permeability and the Forchheimer coefficient are calculated with the following equations with d_p as the mean particle diameter.

$$\kappa = d_p^2 \epsilon_p^3 / \left(150\left(1-\epsilon_p\right)^2\right) \tag{4}$$

$$C_F = 1.75/(\sqrt{150}\epsilon_p^{3/2}) \tag{5}$$

The conservation of species and mass can be written as:

$$\nabla\left[\epsilon_p \rho_f \vec{u}\omega_i - \rho_f \omega_i \sum_k D_{ik}\left(\nabla x_k + \left[x_k - \omega_k\right]\frac{\nabla p}{p}\right)\right] = r_i. \tag{6}$$

In (6) ω_i is the mass fraction of component i, D_{ik} is the binary diffusion coefficient, x_k is the molar fraction of component i and r_i are the consumption or production rates. This is defined based on the reaction rate r_m and the stoichiometric coefficients v_i of the species from (2).

$$r_i = r_m v_i \tag{7}$$

The binary diffusion coefficients are calculated with the Chapman-Enskog theory as detailed in [8] Equation (8) describes the conservation of energy.

$$\nabla\left(\epsilon_p \rho_f \vec{u}\, T\right) = \nabla\left(\lambda_p\left(1-\epsilon_p\right) + \lambda_f \epsilon_p\right) + q_r \tag{8}$$

In (8) T is the temperature, λ_p is the thermal conductivity of the solid particles, λ_f the thermal conductivity of the fluid and q_r is the source term to account for the heat of the reaction with:

$$q_r = r_m(\Delta H^0 + \sum_i v_i c_{p\,i} M_i \left(T - T_0\right)). \tag{9}$$

The fluid density is calculated according to the ideal gas law and the rule of mixture. Values for viscosity and thermal conductivity are calculated for each species with data from [9] as a function of temperature and pressure; the values for the fluid mixture are derived by rule of mixture.

Based on the work of Hwang et al. [10] and Chein et al. [7] the kinetic of the Sabatier-reaction is defined with a Hougen-Watson type rate equation,

$$r_m = \frac{k K_{CO_2} K_{H_2}^4 p_{CO_2} p_{H_2}^4 (1-\beta)}{\left(1 + K_{CO_2} p_{CO_2} + K_{H_2} p_{H_2}\right)^5}. \tag{10}$$

The rate constant k, as well as the equilibrium constants for the surface absorption for each species K_i are calculated with an Arrhenius type equation, the coefficients for (11) are given in Table 1. p_i is the partial pressure of species i in atmospheres and β is the approach-to-equilibrium coefficient defined in (12).

$$k,\, K_i = A \exp\left(-\frac{E_A}{RT}\right) \tag{11}$$

Table 1. Coefficients for the rate constants

Constant	A	E_A
Rate constant, k	1.0635 E11	113.4974 kJ/mol
Adsorption, K_{CO_2}	9.099 E-7	-69.6918 kJ/mol
Adsorption, K_{H_2}	9.6104 E-4	-39.942 kJ/mol

$$\beta = \frac{p_{CH_4} p_{H_2O}^2}{p_{CO_2} p_{H_2}^4 K_{eq}} \tag{12}$$

K_{eq} is the equilibrium constant of the Sabatier reaction defined as:

$$K_{eq} = \exp\left(\frac{28183}{T^2} + \frac{17430}{T} - 8.2536 \log(T) + 2.8032\text{E-}3\ T + 33.165\right) \tag{13}$$

3.2. Domain and boundary conditions of the simulation

The simulated domain is a two dimensional representation of a tubular fixed bed reactor. Fig. 3 shows the simulated geometry and the applied boundary conditions.

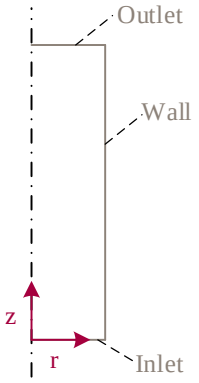

Boundary conditions

Outlet:

$$p = p_R, \frac{\partial \vec{u}}{\partial z} = \frac{\partial T}{\partial z} = \frac{\partial \omega_i}{\partial z} = 0$$

Wall:

$$\vec{u} = 0, \frac{\partial \omega_i}{\partial r} = 0, \left(\lambda_p (1-\epsilon_p) + \lambda_f \epsilon_p\right) \frac{\partial T}{\partial r} = h_W (T - T_C)$$

Inlet:

$$u_r = 0,\ u_z = u_{z\,in}, T = T_{in},\ \omega_i = \omega_{i\,in}$$

Centre axis:

$$\frac{\partial \vec{u}}{\partial r} = \frac{\partial T}{\partial r} = \frac{\partial \omega_i}{\partial r} = 0$$

Fig. 3. Geometry of the simulated domain and the applied boundary conditions.

Table 2 presents all parameters for the simulation and the parameter ranges which were evaluated in the parameter study.

Both the velocity condition at the inlet of the domain, and the composition of the gas mixture at the inlet require further explanation. Under the assumption, that the pressure drop within the reactor is small, the properties of the gas flow at the inlet are calculated with the reactor pressure and the inlet temperature. Further, the hydrogen gas exiting the electrolyser is fully saturated with water. The partial pressure of water in the fully saturated hydrogen equals the vapour pressure in bar and is calculated with the Antoine equation at the temperature of the electrolysis process:

$$p_{H_2O} = \exp\left(5.40221 - \frac{1838.675\ \text{K}}{T_C - 31.737\ \text{K}}\right). \tag{14}$$

The parameters in (14) were taken from [12]. With the partial pressure, the weight fraction at the inlet is:

$$\omega_{H_2O\,in} = \frac{p_{H_2O}}{p_R} \frac{M_{H_2O}}{M_f} = x_{H_2O} \frac{M_{H_2O}}{M_f}, \tag{15}$$

Table 2. Parameters used in the simulation

Parameter	Value	Unit	Reference
Reactor radius, r_R	6 – 20.25	mm	[8]
Reactor length, l_R	254	mm	[4,8]
Mean particle diameter, d_P	0.925	mm	[4]
Bed porosity, ϵ_P	0.35		[4]
Bed thermal conductivity, λ_P	5	W/m/K	[4]
Heat transfer coefficient, h_W	30	W/m²/K	[4]
Coolant temperature, T_C	70	℃	[8]
Inlet temperature, T_{in}	300-500	℃	[4]
Hydrogen inflow, $\dot{V}_{N\,H_2\,in}$	1.1	Nm³/h	[8]
Reactor pressure, p_R	3 – 20	atm	[4, 8]

With the average molar mass M_f. The relative composition of hydrogen to carbon dioxide is fixed as the stoichiometric ratio given in (2), therefore it is defined as:

$$\omega_{H_2\,in}=\left(1-\omega_{H_2O\,in}\right)\frac{|\nu_{H_2}|}{|\nu_{H_2}+\nu_{CO_2}|}, \tag{16 a}$$

$$\omega_{CO_2\,in}=\left(1-\omega_{H_2O\,in}\right)\frac{|\nu_{CO_2}|}{|\nu_{H_2}+\nu_{CO_2}|}. \tag{16 b}$$

As the gas stream at the inlet is not at standard conditions the correct volume flow is calculated with (17) accounting for temperature and pressure, the flux is assumed to be uniform on the entire inlet.

$$\dot{V}_{in}=\dot{V}_{N\,H_2\,in}\frac{|\nu_{H_2}+\nu_{CO_2}|}{|\nu_{H_2}|(1-x_{H_2O})}\frac{T_{in}\,p_0}{T_0\,p_R} \tag{17}$$

3.3. Results

To evaluate the performance of the different reactor geometries and operating conditions studied with the parameter variation the conversion of carbon dioxide is used as the main criterion. It is defined as:

$$X_{CO_2}=\frac{\bar{\omega}_{CO_2\,out}\,\dot{m}_{out}-\omega_{CO_2\,in}\,\dot{m}_{in}}{\omega_{CO_2\,in}\,\dot{m}_{in}}. \tag{18}$$

In Fig. 4 the conversion rate is displayed as a contour plot with reactor radius, inlet temperature and reactor pressure as variables. The reaction kinetics are too slow at low pressure, to result in significant conversion, as Fig. 4(a) shows. This can partly be attributed to the increased water content in the educt gases at lower pressure. Water, or steam, as a product of the Sabatier process (2) will shift the thermodynamic equilibrium of the reaction toward the educts and thereby slow down the reaction. Fig. 4(b) shows that a larger reactor and a higher inlet temperature lead to higher conversion rates. However, below an inlet temperature of 425 ℃ the required conversion of 70 % could not be achieved, regardless of the reactor dimensions. A further interesting point is the large difference in conversion performance a minor change in temperature or reactor radius can cause. This is visualised by the close proximity of the contour lines for 5 and 70 % conversion in Fig. 4(b).

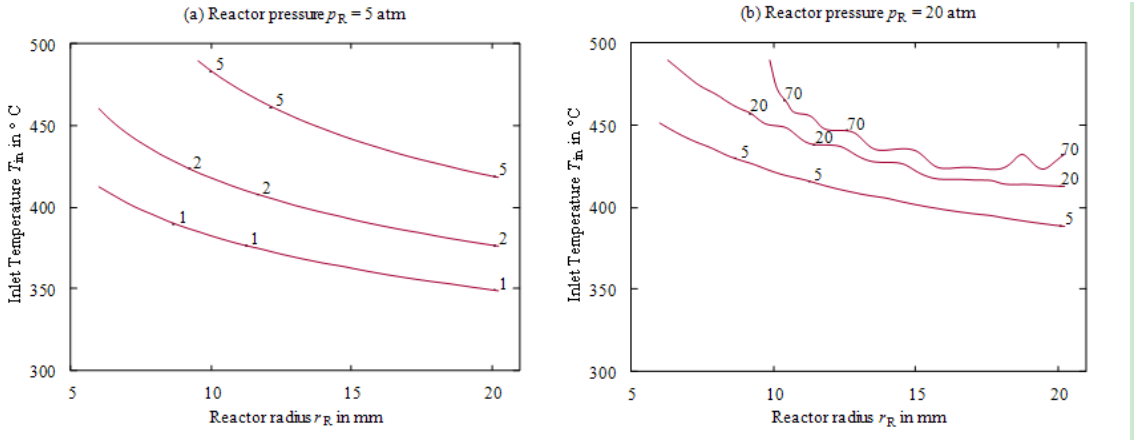

Fig. 4. Contour plots of the conversion X_{CO_2} in percent for a range of reactor geometries and inlet temperatures for two reactor pressures.

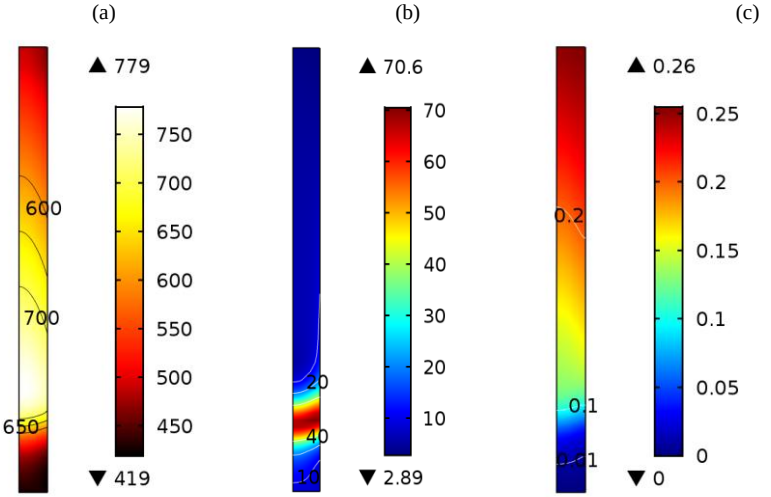

Fig. 5. Distribution of (a) Temperature (℃), (b) reaction rate (mol/m³s) and (c) molar fraction of methane in the reactor with r_R=16.5 *mm* and T_{in}=425 °C.

Fig. 5 (a) shows the temperature profile for the reactor with a radius of 16.5 mm and with an inlet temperature of 425 ℃. It can be seen that a hot zone exists, where the temperatures exceed 700 ℃. Behind the hot zone the reactor temperature drops down to around 500 ℃ at the outlet. This temperature profile is expected in fixed bed reactors. At the start of the hot zone the high temperature enables fast reaction kinetics. In this region the respective balance between the educts and products of the reaction is strongly on the product side, due to the high concentrations of the educts at the inlet. Further, the temperature provides the required activation energy without limiting the conversion due to the thermodynamic equilibrium. Fig. 5 (c) shows the molar fraction of methane increases from 0.01 to 0.1 through the initial reaction zone. However, the further conversion up to a molar fraction of 0.2 at the outlet is realised in the rear part of the reactor with very slow reaction kinetics. In the rear part of the reactor the thermodynamic equilibrium of the Sabatier process is again shifted toward the products due to the lower temperature improving the selectivity of the overall reaction toward methane production.

4. Conclusion and Outlook

The EMC as a possible concept to improve the efficiency and profitability of PtG systems has been introduced. A number of requirements for the performance of an EMC have been defined and the resulting requirements for the reactor were derived. Based on a thermochemical model the performance of a fixed bed reactor in an EMC has been studied. A parameter study on reactor pressure, radius and inlet temperature was done. With the simple fixed bed reactor layout a minimal inlet temperature of 425 ℃ was found to achieve the required conversion of CO_2. However, both the required inlet temperature and the high temperatures within the reactor due to the exothermic reaction are not ideal for an integration into an EMC. These high temperature differences would lead to significant thermal expansion and therefore mechanical tension within the structure of the EMC.

Another reactor concept using a dielectric barrier discharge plasma could offer better properties for the integration in EMC. Nizio et al. [13, 14] were able to show high conversion rates at moderate temperatures and *GHSV* in excess of 40,000 h^{-1}. The non-thermal plasma created by a dielectric barrier discharge can produce the reactive species necessary for the Sabatier-Reaction without the need for high temperatures. Ashford et al. studied the dynamic abilities of a plasma reactor and found that the plasma can offer a possible control function to alter the reaction rate within the reactor according to the load [15]. This would be a useful ability for start-up of the EMC and the operation under constantly fluctuating conditions.

Therefore, the authors are planning to investigate high-pressure hybrid-plasma-catalytic-reactors for the application in EMC.

Acknowledgements

The work is conducted in the project “Development and Test of electrically controllable Membrane Units in Polymer Electrolyte Fuel Cells and Electrolysers with an internal Methanation in the gas exhaust pipe“ funded by the BMWi (funding code 03ET6133A) and in cooperation with Altran.

References

[1] Schaaf T, Grünig J, Schuster MR, Rothernfluh T, and Orth A. Methanation of CO_2 - storage of renewable energy in a gas distribution system. *Energ Sustain Soc*, 4(2).

[2] Physikalisch-Technische Bundesanstalt, “Einspeisung von Biogas in das Erdgasnetz (engl. Supply of biogas to the gas grid),“ Technical regulations, G 14, Nov. 2007.

[3] Schulz D. High efficiency fuel cell, European Patent, EP2978875, Mar. 25th, 2014.

[4] Schulz D. High efficiency fuel cell, United States Patent, No. US 1050235506 B2, July 2018.

[5] Schulz D. High efficiency fuel cell, Japanese Patent, No. 6462660, Jan. 2019.

[6] Schulz D. High efficiency fuel cell, Chinese Patent, No. ZL 2014800178483, June 2018.

[7] Chein RY, Chen WY, Yu CT. Numerical simulation of carbon dioxide methanation reaction for synthetic natural gas production in fixed-bed reactors. *J. of Nat. Gas Sc. and Engineering*, Feb. 2016; 29: 243-251.

[8] Bird RB, Stewart WE, and Lightfoot EN. *Transport Phenomena*, 2nd ed., New York: Wiley, 2002.

[9] VDI-Gesellschaft Verfahrenstechnik und Chemieingenieurwesen, VDI Heat Atlas, 11th ed., Berlin: Springer-Vieweg, 2013.

[10] Hwang S, Hong UG, Lee J, Baik JH, Koh DJ, Lim H and Song IK. Methanation of carbon dioxide over Mesoporous Nickel–M–Alumina (M = Fe, Zr, Ni, Y, and Mg) Xerogel Catalysts: Effect of second metal. *Catal. Lett.*, vol. 142, May 2012, pp. 2012

[11] H-TEC Systems, “H-TEC Series-S: S 30/30,” [Online]. Available: https://www.h-tec-systems.com [Accessed: June 26, 2019]

[12] Bridgeman OC and Aldrich EW. Vapor pressure tables for water. *J. Heat Transfer*, 1964; 86: 279-286.

[13] Nizio M, Benrabbah R, Krzak M, Debek R, Motak M, et al. Low temperature hybrid plasma-catalytic methanation over Ni-Ce-Zr hydrotalcite-derived catalysts. *Catalysis Communications*, 2016; 83: 14-17.

[14] Nizio M, Albarazi A, Cavadias S, Amouroux J, Galvez ME, et al. Hybrid plasma-catalytic methanation of CO_2 at low temperature over ceria zirconia supported Ni catalysts. *Int. J. of Hydrogen Energy*, July 2016; 41: 11584-11592.

[15] Ashford B und Tu X. Non-thermal plasma technology for the conversion of CO_2. *Current Opinion in Green and Sustainable Chemistry*, Feb. 2017; 3: 45-49.